

**Low dose IL-17 therapy prevents and reverses diabetic nephropathy, metabolic syndrome and associated organ fibrosis**

Riyaz Mohamed<sup>1</sup>  
Calpurnia Jayakumar<sup>1</sup>  
Feng Chen<sup>1</sup>  
David Fulton<sup>1</sup>  
David Stepp<sup>1</sup>  
Ron T. Gansevoort<sup>2</sup>  
Ganesan Ramesh<sup>1</sup>

Department of Medicine and Vascular Biology Center  
Georgia Regents University  
Augusta, GA 30912.

<sup>2</sup>Department of Physiology  
Georgia Regents University  
Augusta, GA 30912

<sup>3</sup>Department of Nephrology, University Medical Center Groningen, University of Groningen,  
Groningen, The Netherlands

**RUNNING TITLE:** IL-17 and Diabetic Nephropathy

**Correspondence Address:**

Ganesan Ramesh, Ph.D.

Department of Medicine and Vascular Biology Center, CB-3702

Georgia Regents University

1459 Laney-Walker Blvd

Augusta, GA 30912

TEL. NO. (706) 721-9728

FAX. NO. (706) 721-9799

E-mail: [gramesh@gru.edu](mailto:gramesh@gru.edu)

## Supplementary Figure S1.

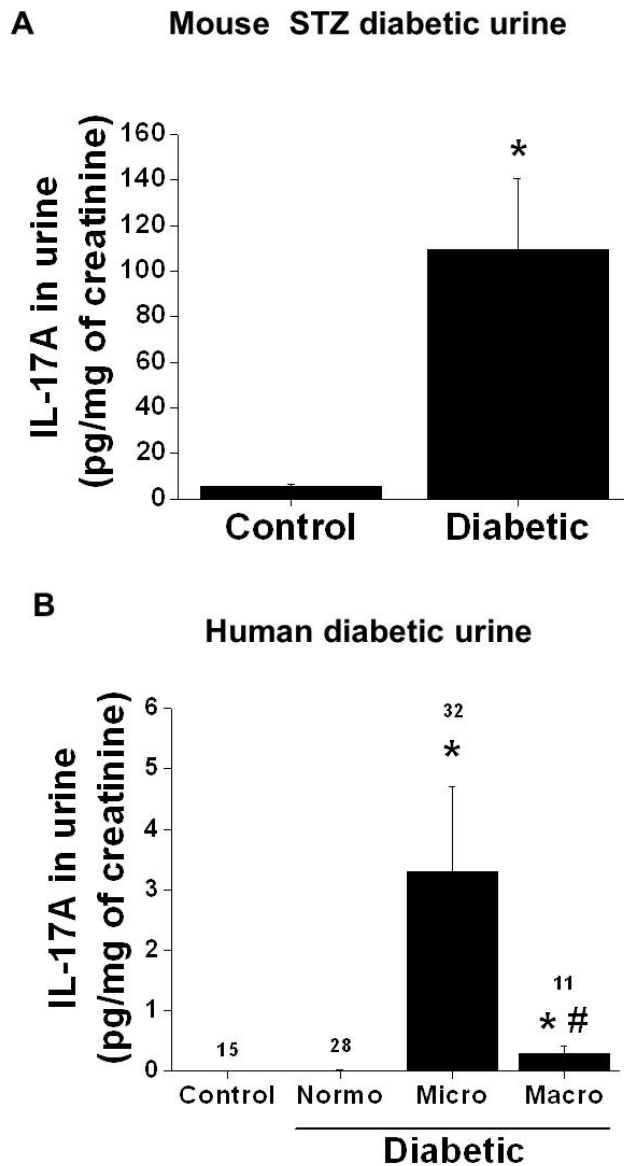
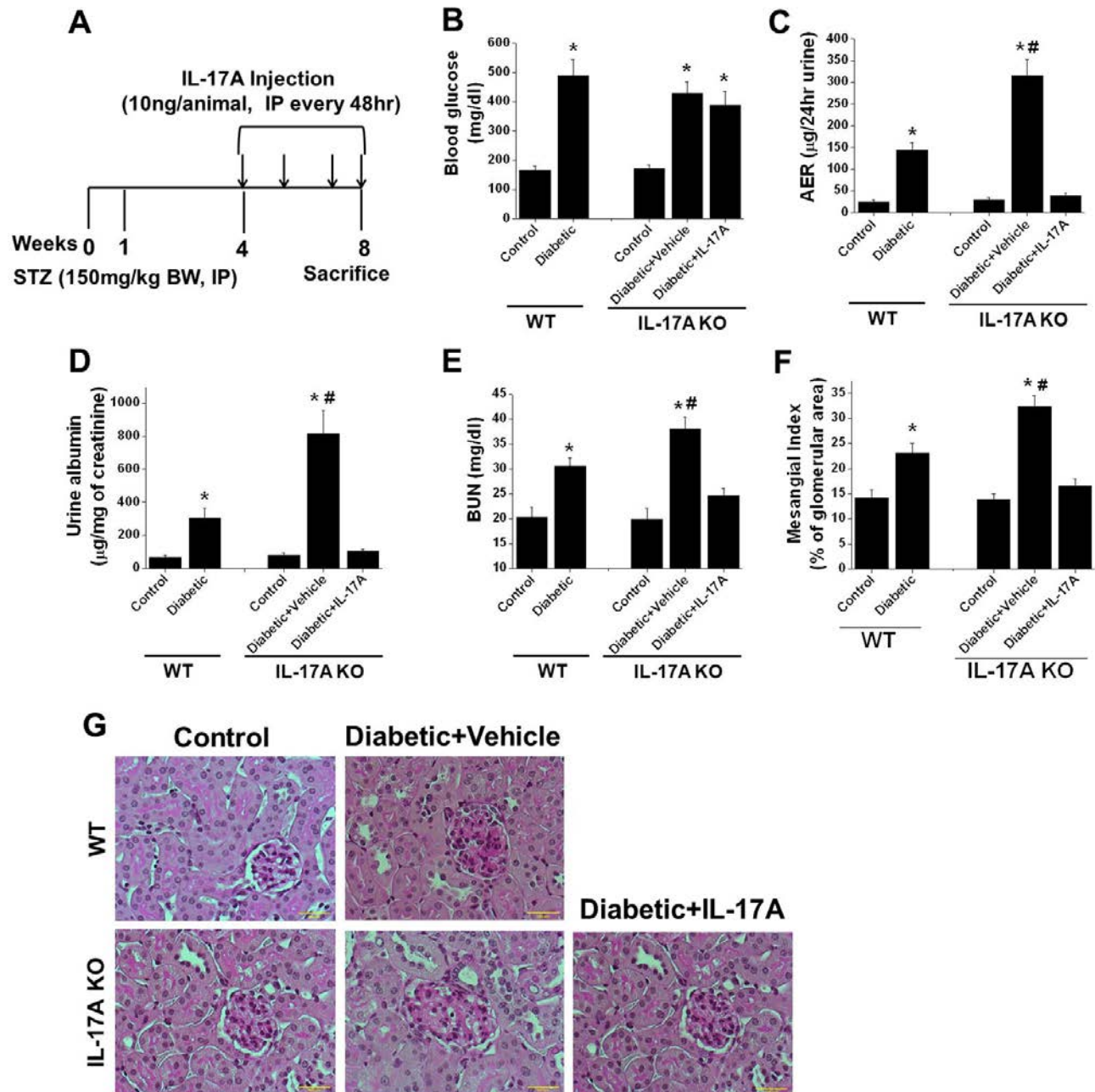


Figure S1. Quantification of IL-17A excretion in diabetic mouse (STZ induced) and human patients. IL-17A was quantified by ELISA. IL-17A excretion was significantly increased after 8 weeks of diabetes over non-diabetic control mouse. \*,  $p < 0.001$  vs. control.  $n = 8-10$ . Excretion of IL-17A in healthy control and diabetes without microalbuminuria (normo) showed low levels of IL-17A excretion, which was significantly increased in patients with microalbuminuria and macroalbuminuria. However, macroalbuminuria patients had significantly lower levels of IL-17A as compared to microalbuminuria patients. \*,  $p < 0.05$  vs. other groups. #,  $p < 0.05$  vs. microalbuminuria group. Number patients analyzed in each group is indicated at top of each bar.

## Supplementary Figure S2.



**Figure S2.** IL-17A administration to diabetic IL-17A knockout mice suppresses diabetic nephropathy. A. Diabetes was induced by administering a single dose of STZ, and 4 weeks after induction of diabetes, animals were received either vehicle or IL-17A for additional 4 weeks (10ng/animals/every 48hr). Animals were sacrificed at 8 weeks after induction of diabetes and tissues were processed for histopathology. B. Blood glucose in WT and IL-17A knockout (KO) mice. \*,  $p < 0.001$  vs. control. C. Albumin excretion rate in WT and IL-17A KO diabetic mice. \*,  $p < 0.001$  vs. control. #,  $p < 0.05$  vs. vehicle treated IL-17A KO diabetic. D. Albumin excretion normalized to mg of creatinine. \*,  $p < 0.01$  vs. control. #,  $p < 0.05$  vs. vehicle treated IL-17A KO diabetic. E. Renal function was

determined by measuring blood urea nitrogen (BUN). \*,  $p < 0.05$  vs. control. #,  $p < 0.05$  vs. vehicle treated IL-17A KO diabetic. F. Quantification of mesangial expansion. \*,  $p < 0.05$  vs. control. #,  $p < 0.05$  vs. WT diabetic. #,  $p < 0.001$  vs. vehicle treated IL-17A KO diabetic. G. PAS stained section from WT and IL-17A KO control and diabetic mice treated with vehicle or IL-17A. Diabetes induced glomerular hypertrophy and mesangial expansion in WT mice and IL-17A KO mice which was suppressed in IL-17A treated IL-17A KO mice kidney. Scale bar: 100  $\mu$ M. N=6.

### Supplementary Figure S3.

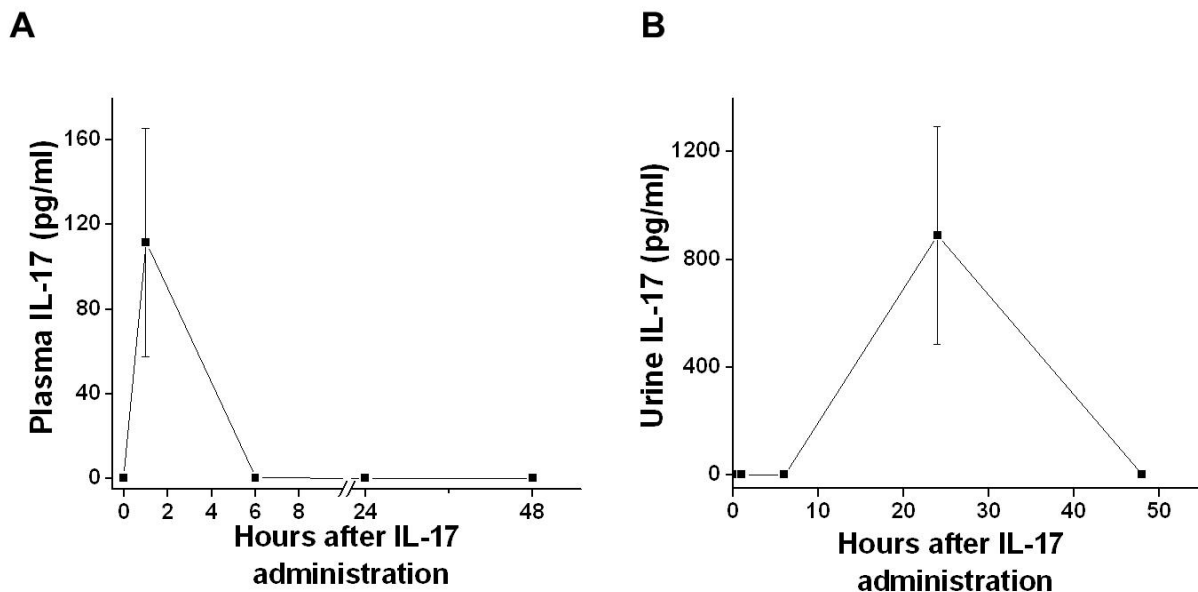


**Figure S3. IL-17A plasma clearance kinetics in WT mice.** 10ng of recombinant IL-17A was administered intraperitoneally, after which blood (A) and urine (B) samples were collected at various time points. Plasma and urine IL-17A were quantified by ELISA as described in Materials and Methods.

**Supplementary Table S1. Effect of IL-17 isoforms at different doses on diabetes induced albuminuria, polyuria, kidney weight/body weight ratio and blood glucose**

Animals (number of animal)	Treatment	Blood glucose (mg/dl)	Urine glucose (mg/dl)	Urine Volume (ml)	KW/BW¶ (mg/gm)	Urine albumin (µg/24hr)
Non-Diabetic (12)	Vehicle	198±11	98±12	0.8±0.2	9±1	24±5
Non-Diabetic (5)	IL-17A	205±9	61±10	0.9±0.2	10±0.1	19±3
Diabetic (15)	Vehicle	634±115*	10900±1648*	26±6*	16±2*	200±7*
Diabetic (12)	10ng IL-17A	622±43*	10144±667*	24±3*	13±1	110±12*#
Diabetic (6)	50ng IL-17A	512±132*	14225±2345*	31±5*	14±2	98±4*#
Diabetic (6)	100ng IL-17A	480±55*	12240±912*	18±6*	15±1*	109±36*#
Diabetic (6)	10ng IL-17E	630±66*	11650±2847*	20±5*	13±1	233±44*
Diabetic (6)	10ng IL-17F	576±101*	8860±1786*	18±6*	15±2*	128±29*#
Diabetic (6)	10ng IL-17C	658±17*	11067±1768*	18±3*	15±1*	283±74*

\*,  $p < 0.05$  vs. Non diabetic vehicle or IL-17A treated.

#,  $p < 0.05$  vs. Diabetic vehicle treated.

¶, kidney weight/body weight ratio.

# Supplementary Figure S4.

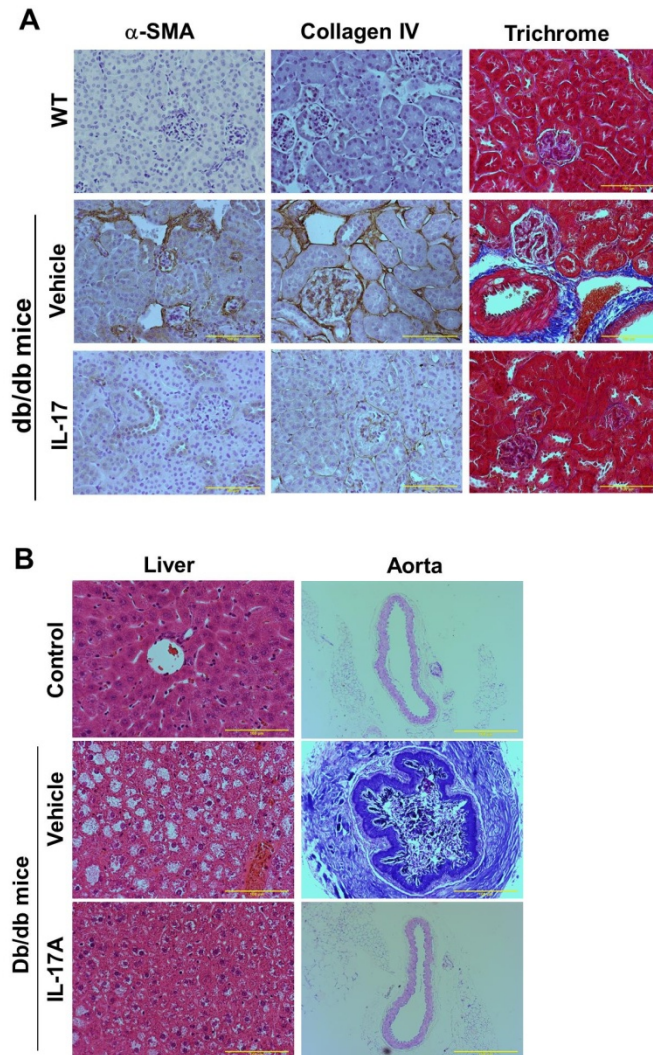


**Figure S4.** Fibrosis was determined by immunohistochemical staining for  $\alpha$ -SMA, collagen IV and Masson's trichrome staining. Scale bar: 100  $\mu$ M. Vehicle treated diabetic mouse kidney shows increased expression of  $\alpha$ -SMA, collagen IV and trichrome staining, which was reduced in IL-17A treated mouse kidney. B. Lipid deposition and fibrosis in liver was determined by Masson's trichrome staining. Scale bar: 100  $\mu$ M. Fat deposition in and around the aorta was determined by Toluidine blue staining. Vehicle treated liver and aorta show a large amount of lipid deposition that was entirely suppressed in IL-17A treated db/db mice.

## Supplementary Figure S5.

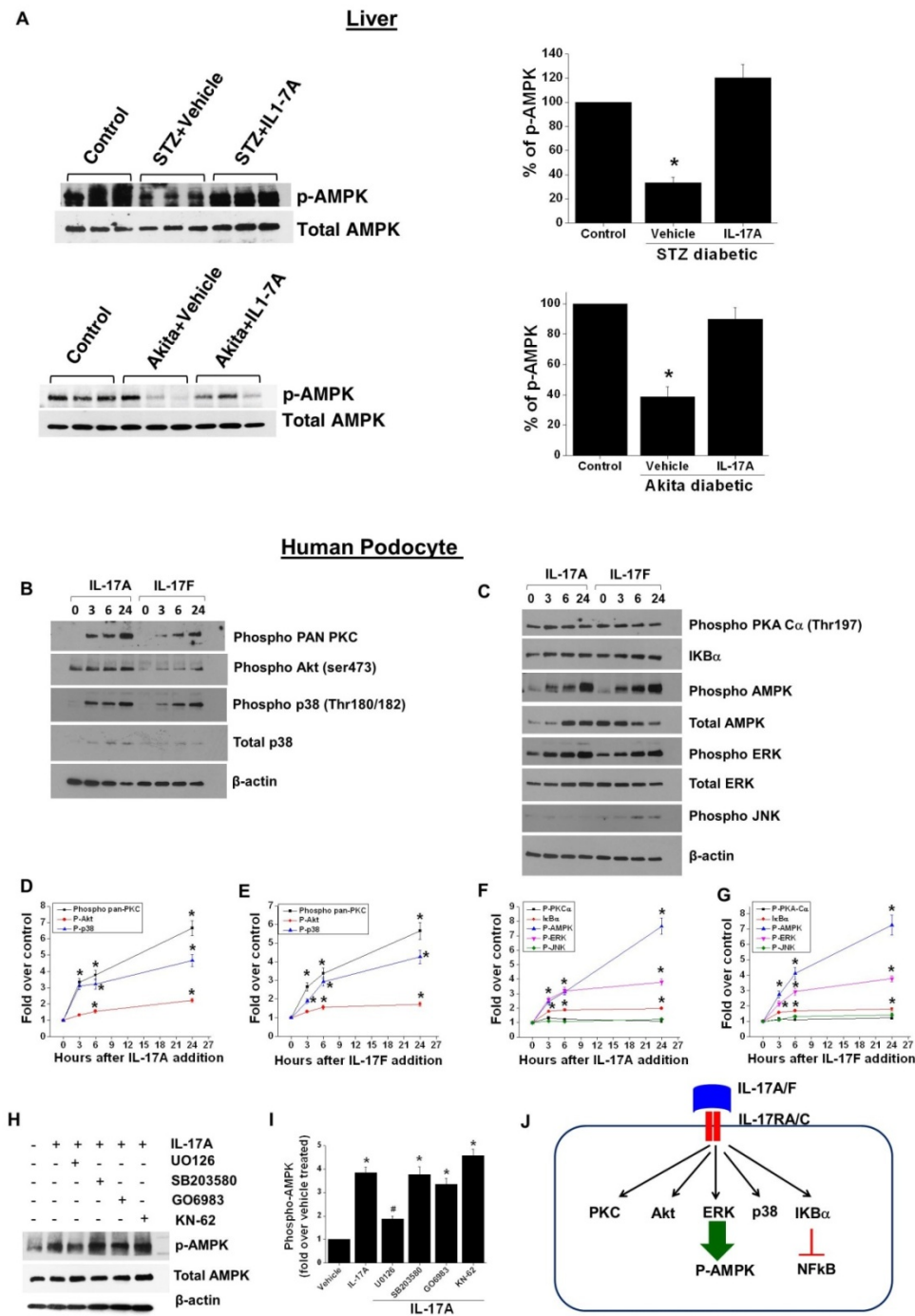


**Figure S5. IL-17A administration suppresses diabetes induced downregulation of AMPK activation in liver (A) and increases AMPK activation through ERK MAPK (B-J) in human podocytes.** A. Western blot analysis of phosphor and total AMPK in control and diabetic animals (left panel) and densitometric quantification of AMPK expression (right panel). \*,  $p < 0.001$  vs. other groups. B & C. Western blot analysis of



phosphorylation of different kinases in podocytes in response to IL-17A or IL-17F treatment (50ng/ml) at different time points. D-G. Quantification of Western blots by densitometry. Phospho kinase levels were expressed as a fold increase over control, and protein loading was normalized to total kinase and actin level. \*,  $p < 0.05$  vs. control (0hr). n=4. H-I. ERK pathway inhibitor (U0126) but not p38 (SB203580) or PKC (GO6983) or calmodulin kinase (KN-62) inhibitor suppressed IL17A induced AMPK phosphorylation, suggesting in part that ERK is an upstream activator of AMPK. \*,  $p < 0.001$  vs. vehicle treated. #,  $p < 0.05$  vs. IL-17A treated. n=3. J. Schematic representation of IL17A/F mediated activation of AMPK in human podocytes.

**Supplementary Figure S6.**

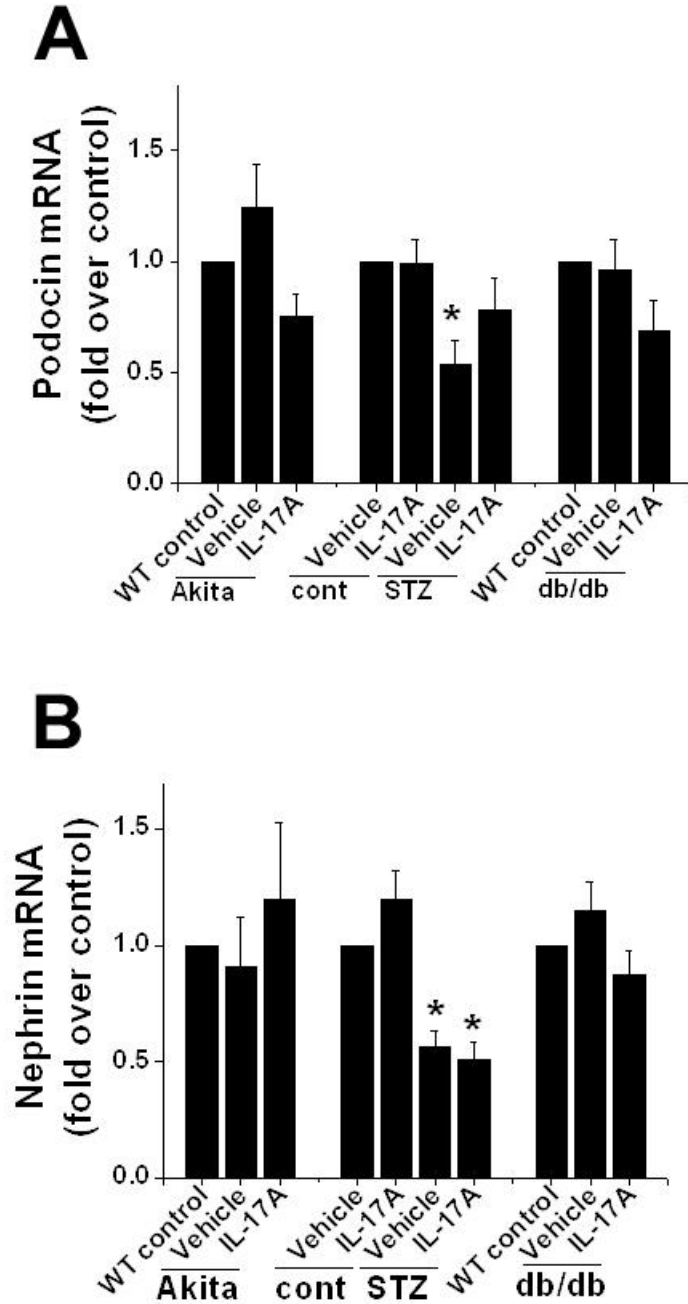


**Figure S6.** Quantification of podocin and nephritin mRNA in the diabetic mouse kidney by real time RT-PCR analysis. Kidney from WT, Ins2Akita, db/db and STZ diabetic mice that are treated with vehicle or IL-17A as described in Materials and Methods were used for mRNA quantification. \*,  $p < 0.05$  vs. control. N=4-6.

**Supplementary Figure S7.**

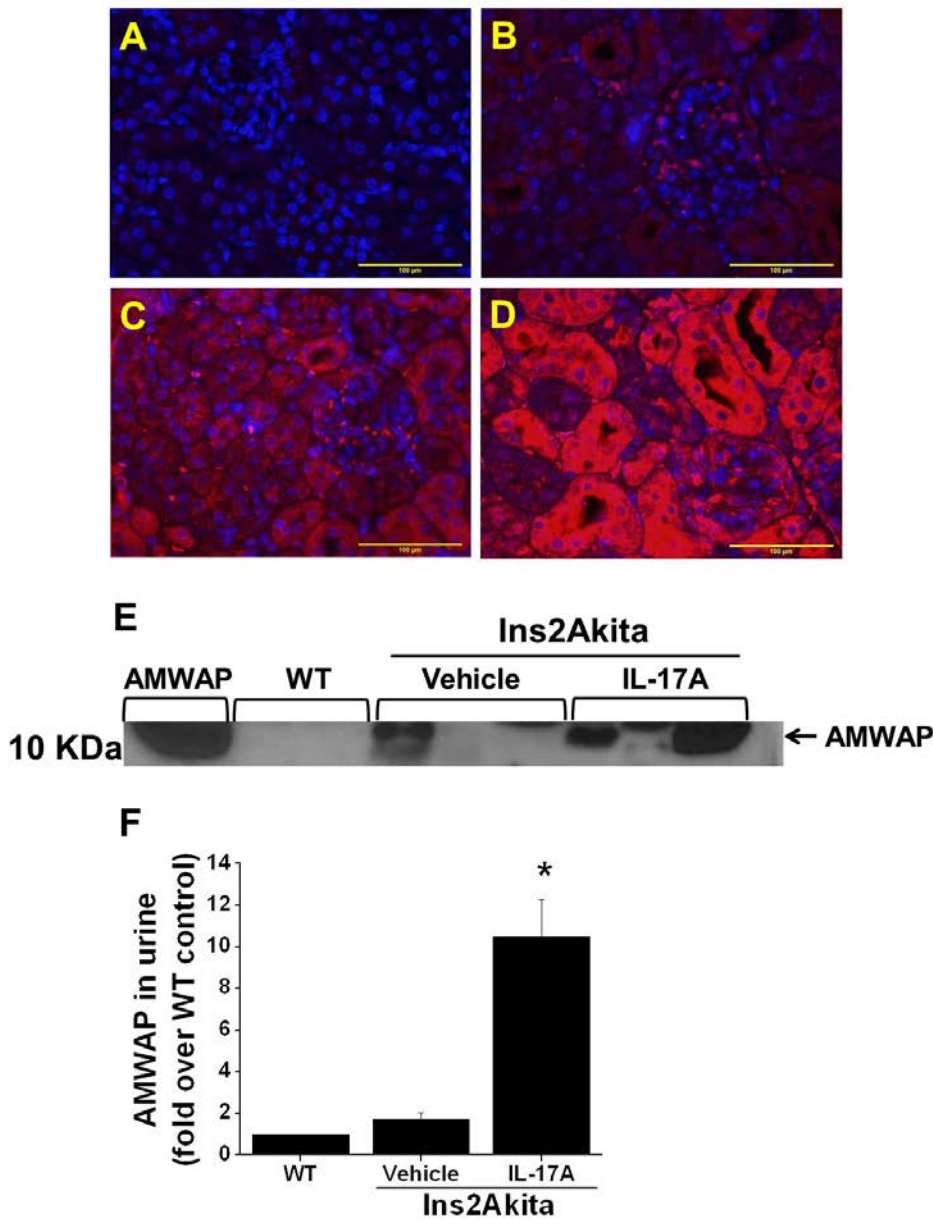


**Figure S7. AMWAP immunolocalization in the kidney.** A. 2<sup>nd</sup> antibody control. B. Wild type non-diabetic control. C. Vehicle treated Ins2Akita mouse kidney. D. IL-17A treated Ins2Akita mouse kidney showing intense staining in the tubular epithelium and podocytes. Scale bar: 100  $\mu$ M. E. Western blot analysis of AMWAP excretion in urine from WT, vehicle and IL-17A treated Ins2Akita mice. F. Densitometric quantification of AMWAP Western blots. \*,  $p < 0.001$  vs. other groups.  $n = 4-6$ .

## Supplementary Figure S8.

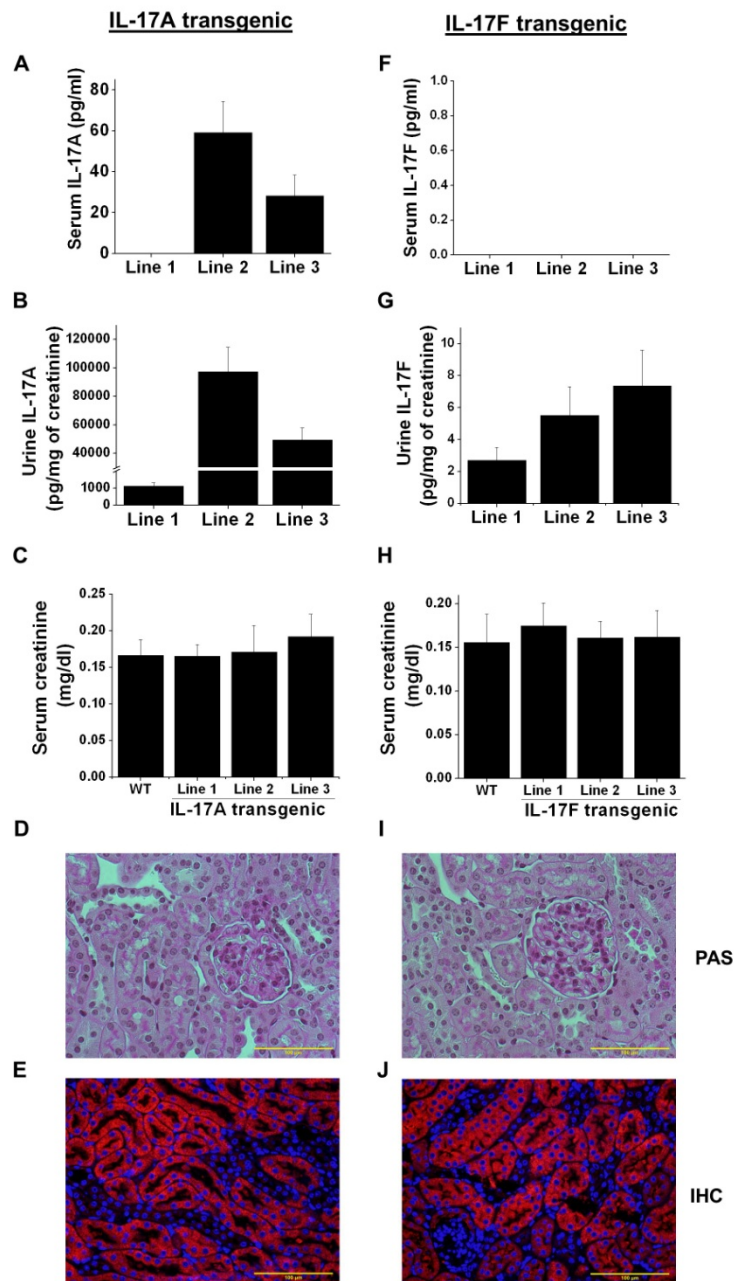


**Figure S8.** Characterization of 12 weeks old IL-17A (A-E) transgenic mice and IL-17F (F-J) transgenic mice for transgene expression and kidney function. A. Quantification of IL-17A levels in serum by ELISA. B. Quantification of IL-17A levels in urine by ELISA. C. Kidney function was determined by measuring serum creatinine. D. PAS-hematoxylin stained kidney section showing normal morphology. E. Immunohistochemical localization of IL-17A in line 2 kidney. Characterization of 12-week old IL-17A (F-J) transgenic mice. A. Quantification of IL-17F levels in serum by ELISA. B. Quantification of IL-17F levels in urine by ELISA. C. Kidney function was determined by measuring serum creatinine. D. PAS-hematoxylin stained kidney section showing normal morphology. E. Immunohistochemical localization of IL-17F in line 2 kidney. Scale bar: 100  $\mu$ M. N=6-8.

## Supplementary Figure S9.

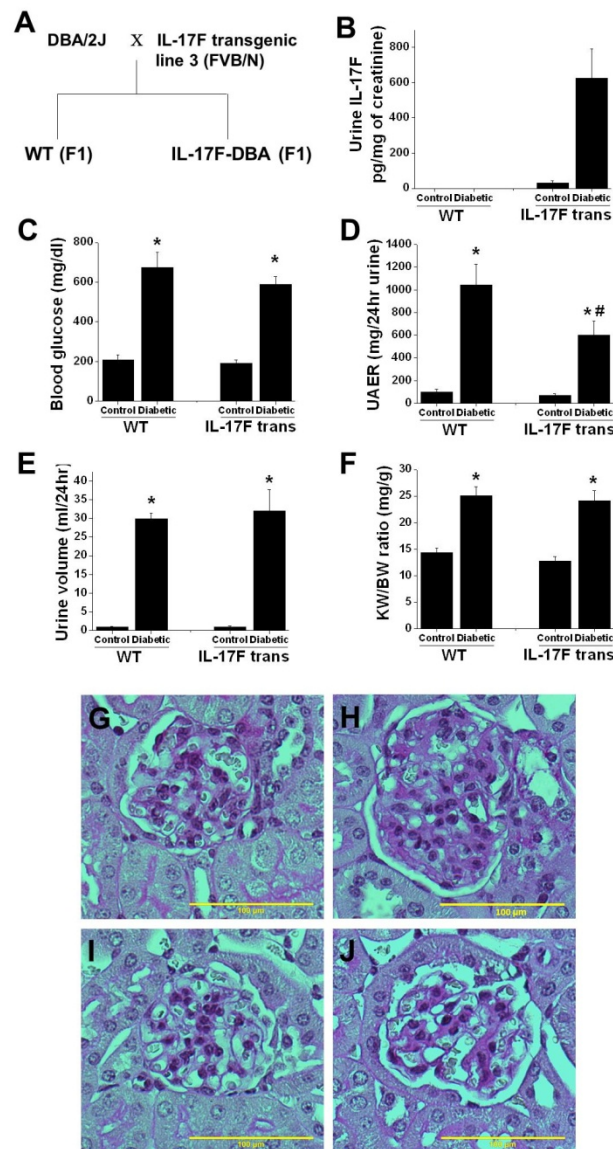


**Figure S9.** Epithelial specific overexpression of IL-17F is sufficient to suppress diabetic nephropathy. Data from Line 3. **A.** IL-17F transgenic mice were crossed with nephropathy prone strain DBA/2J. 6-week old WT and IL-17A positive F1 mice were given a single dose of STZ (150mg/kg BW). Mice were sacrificed 8 weeks after STZ administration, and albuminuria was quantified. **B.** Quantification of IL-17F excretion in urine. IL-17F is only detectable in IL-17F transgenic mouse urine but not in plasma (not shown). **C.** Blood glucose level at 8 weeks of diabetes. **D.** Urine albumin excretion rate (UAER) expressed as microgram per 24hr urine. **E.** Urine volume per 24hr. **F.** Kidney hypertrophy was calculated as ratio of kidney weight and body weight (KW/BW). **G-J.** PAS-hematoxylin stained kidney section. **G.** WT control. **H.** WT diabetic. **I.** IL-17F transgenic control. **J.** IL-17A transgenic diabetic mouse kidney. Scale bar: 100  $\mu$ M. \* $p$ <0.001 vs. other groups. #,  $p$ <0.05 vs. WT diabetic. N=8-12.

**Supplementary Table 2. Plasma lipid profile from WT and IL-17A transgenic mice in a mixed background (FVB/N vs. DBA/2J).**

Animals	Treatment	Triglycerides (mg/dl)	HDL (mg/dl)	LDL/VLDL (mg/dl)	Total cholesterol (mg/dl)
WT	Non-diabetic	254±17	108±15	29±2	90±17
WT	Diabetic	390±26*	67±17*	33±5	83±17
IL-17A (line 1)	Non-diabetic	278±33	105±4	29±3	114±16
IL-17A (line 1)	Diabetic	163±31 <sup>#</sup>	92±6	21±5	95±16
IL-17A (line 2)	Non-diabetic	303±24	109±8	33±5	104±19
IL-17A (line 2)	Diabetic	220±29 <sup>#</sup>	88±9	20±5 <sup>\$</sup>	97±22
IL-17F (line 3)	Non-diabetic	317±21	99±13	30±2	107±9
IL-17F (line 3)	Diabetic	223±19 <sup>#</sup>	81±8	26±3	87±5

6-week old transgenic and WT mice were made diabetic with a single dose of STZ. Animals were sacrificed at 8 weeks after induction of diabetes, and plasma lipid levels were quantified. \*,  $p < 0.01$  vs. non-diabetic control. #,  $p < 0.001$  vs. WT diabetic and corresponding transgenic non-diabetic controls. \$,  $p < 0.05$  vs. line 2 non-diabetic control and WT diabetic. N=6-8.

**Supplementary Figure S10.**

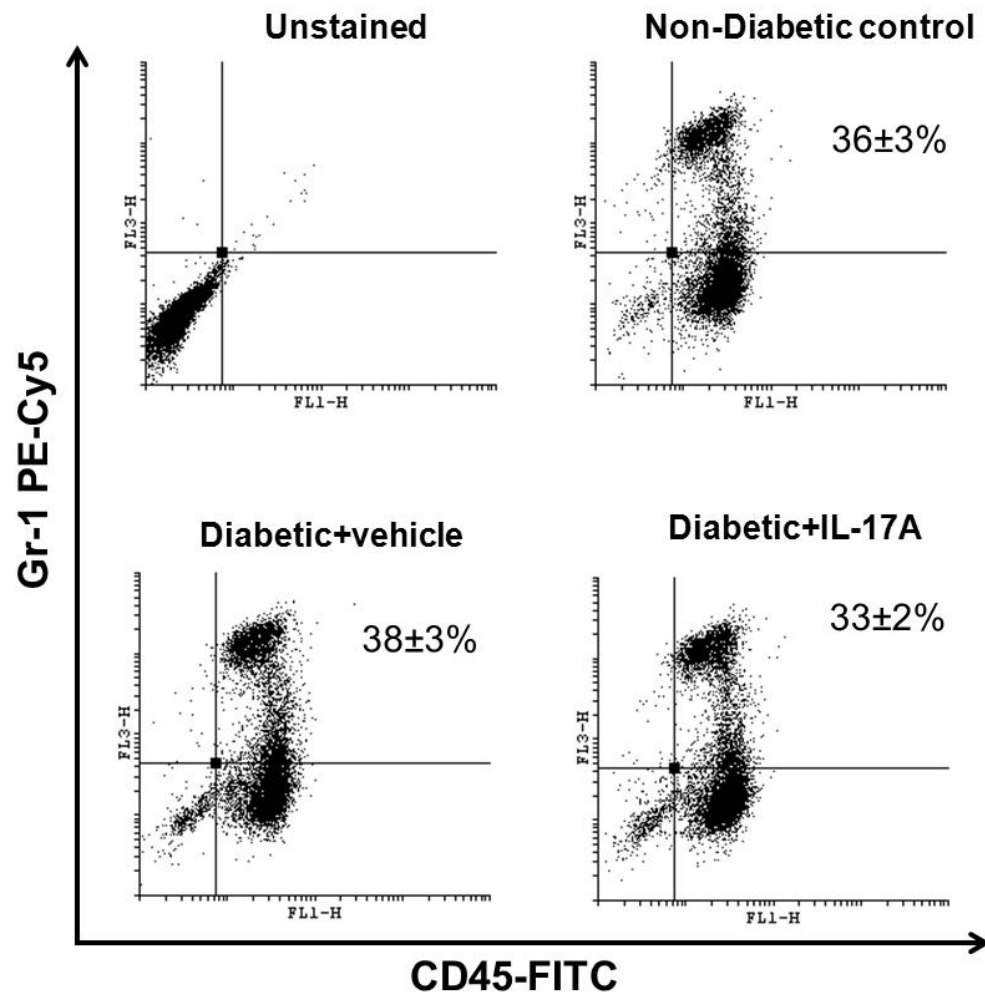


**Figure S10.** Flow cytometric analysis of neutrophils in blood from non-diabetic control mice, vehicle-treated diabetic mice and diabetic mice treated for 6 week with IL-17A (10ng/animal). N=4.

**Supplementary Figure S11.**

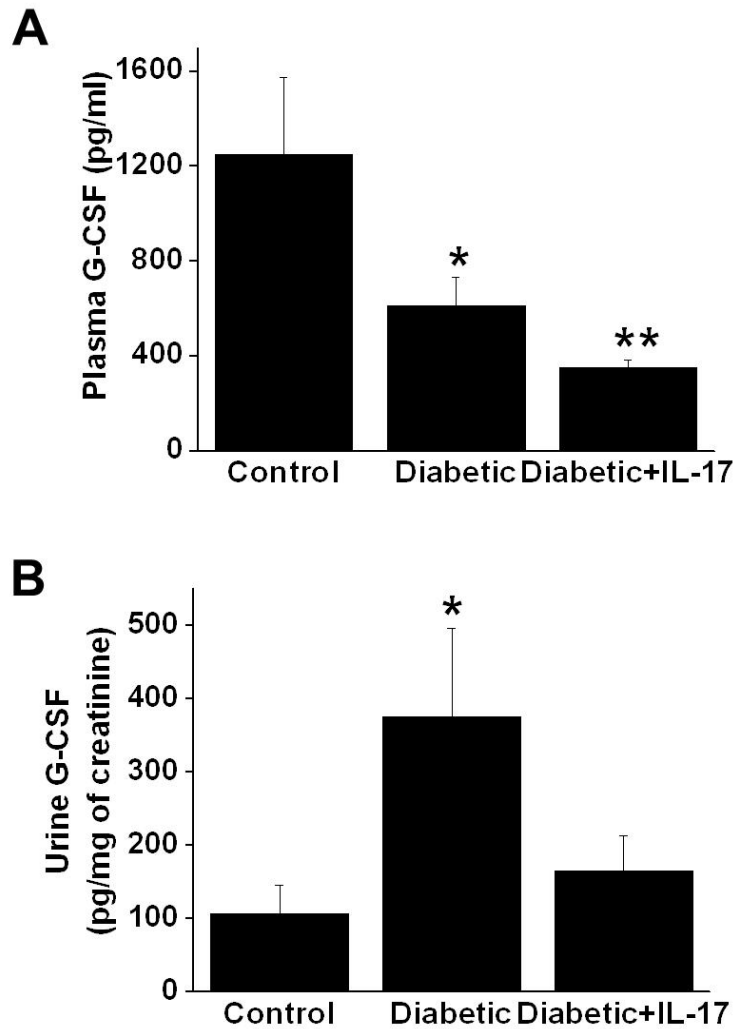


**Figure S11.** Quantification of plasma and urine granulocyte colony stimulating factor (G-CSF) by ELISA in control and diabetic animals treated with vehicle or IL-17A. Diabetes was induced by administering STZ, and G-CSF was quantified at 12 weeks after STZ administration. \*,  $p < 0.001$  vs. other groups. \*\*,  $p < 0.05$  vs. diabetic animals. N=4-6.



Supplementary Figure S12.

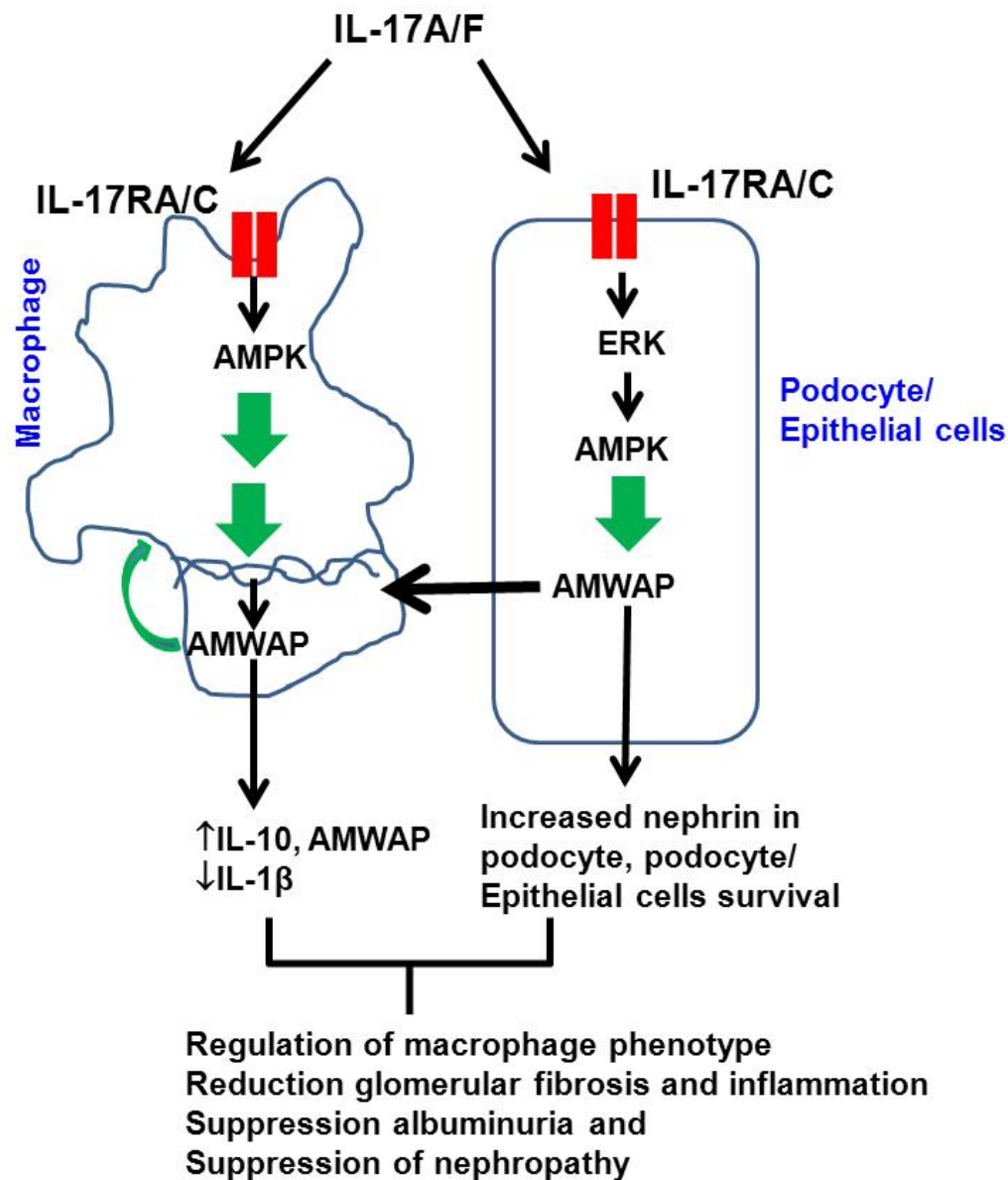


**Figure S12.** Model depicts the pathways through which IL-17A/F may protect kidney against diabetic nephropathy. IL-17A/F may act through IL-17RA and IL-17RC in macrophage, podocyte and epithelial cells. Binding of IL-17 to its receptors causes the activation of AMPK in an ERK MAPK dependent manner which then may increase the AMWAP expression. AMWAP, acting in autocrine or paracrine manner, will increase IL-10 production and suppression of macrophage inflammatory phenotype. AMPK may also increase podocyte survival independent of AMWAP. Together, IL-17A/F suppresses diabetic nephropathy.